HHS Public Access

Author manuscript

Mater Horiz. Author manuscript; available in PMC 2020 August 28.

Published in final edited form as:

Mater Horiz. 2019 ; 6(8): 1625–1631. doi:10.1039/c9mh00375d.

Individual cell-only bioink and photocurable supporting medium for 3D printing and generation of engineered tissues with complex geometries†

Oju Jeon[a,1,*], **Yu Bin Lee**[a,1,*], **Hyoen Jeong**[a], **Sang Jin Lee**[a,1], **Derrick Wells**[a,1], **Eben Alsberg**[a,b,1,2]

[a]Department of Biomedical Engineering, Case Western Reserve University, Cleveland, OH 44106.

[b]Department of Orthopaedic Surgery, Case Western Reserve University, Cleveland, OH 44106.

Abstract

Scaffold-free engineering of three-dimensional (3D) tissue has focused on building sophisticated structures to achieve functional constructs. Although the development of advanced manufacturing techniques such as 3D printing has brought remarkable capabilities to the field of tissue engineering, technology to create and culture individual cell only-based high-resolution tissues, without an intervening biomaterial scaffold to maintain construct shape and architecture, has been unachievable to date. In this report, we introduce a cell printing platform which addresses the aforementioned challenge and permits 3D printing and long-term culture of a living cell-only bioink lacking a biomaterial carrier for functional tissue formation. A biodegradable and photocrosslinkable microgel supporting bath serves initially as a fluid, allowing free movement of the printing nozzle for high-resolution cell extrusion, while also presenting solid-like properties to sustain the structure of the printed constructs. The printed human stem cells, which are the only component of the bioink, couple together via transmembrane adhesion proteins and differentiate down tissue-specific lineages while being cultured in a further photocrosslinked supporting bath to form bone and cartilage tissue with precisely controlled structure. Collectively, this system, which is applicable to general 3D printing strategies, is a paradigm shift for printing of scaffold-free individual cells, cellular condensations and organoids, and may have far reaching impact in the fields of regenerative medicine, drug screening, and developmental biology.

Graphical Abstract

Functional engineered tissue structures with complex geometries can be created by 3D bioprinting of individual cell-only bioinks into a photocrosslinkable microgel supporting bath, which permits precise structural control over cellular condensation formation and long-term culture.

---

†Electronic Supplementary Information (ESI) available: [details of any supplementary information available should be included here]. See DOI: 10.1039/C9MH00375D

[1]Current Address: Department of Bioengineering, University of Illinois at Chicago, Chicago, IL 60607
[2]Current Address: Department of Orthopaedics, University of Illinois at Chicago, Chicago, IL 60607
*These authors equally contributed to this work.

Conflicts of interest
There are no conflicts to declare.

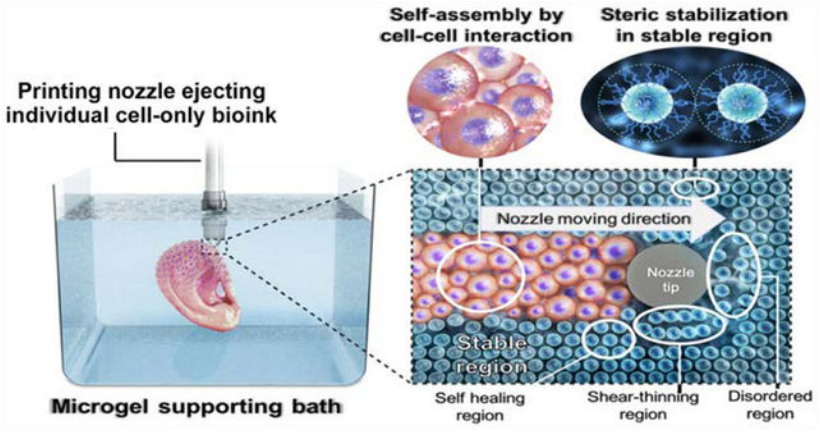

Introduction

Over the past decades, scaffolding approaches have been widely used to create functional tissues or organs in tissue engineering and regenerative medicine fields.[1] However, the use of biomaterial-based scaffolds faces several challenges, such as interference with cell-cell interactions, potential immunogenicity of the materials and their degradation byproducts, unsynchronized rates of scaffold degradation with that of new tissue formation, and inhomogeneity and low density of seeded cells.[2] To overcome these limitations of scaffold-based approaches, scaffold-free tissue engineering has recently emerged as a powerful strategy for constructing tissues using multicellular building blocks that self-assemble into geometries such as aggregates, sheets, strands and rings.[3] These building blocks have been organized and fused into larger and more complicated structures, sometimes comprised of multiple cell types, and then they produce extracellular matrix (ECM) to form mechanically functional three-dimensional (3D) tissue constructs.[4–6] However, it is still difficult to precisely control the architecture and organization of cell-only condensations to mimic sophisticated 3D structures of natural tissues and their structure-derived functions.

Recently, 3D printing has been applied in tissue engineering with the potential to create complicated 3D structures with high resolution using cell-free or cell-laden bioinks.[7] Digital imaging data, obtained from computed tomography scans and magnetic resonance imaging, provide instruction for the desired geometry of printed constructs.[7, 8] Biodegradable thermoplastics, such as polycaprolactone, polylactic acid, and poly(lactic-co-glycolic acid), are advantageous for printing as stable constructs with delicate structural control can be formed due to the mechanical integrity of original materials.[9–11] However, a major drawback is that cells cannot be printed simultaneously due to the use of organic solvents or high temperature to extrude the polymer inks.[12] In contrast, materials that form cytocompatible and biocompatible hydrogels, such as alginate, gelatin, collagen, hyaluronic acid and polyethylene glycol, have been explored as prospective bioinks due to the feasibility of encapsulating cells within them during the printing process to provide a 3D cellular milieu.[7, 13–15] However, the hydrogel-based bioinks present the aforementioned limitations of scaffolding-based strategies. Since there has not been a platform enabling the printing and long-term culture of individual single cells while maintaining their resulting printed spatial

position without incorporation of biomaterials, 3D cell printing in a scaffold-free manner has rarely been achieved. Bhattacharjee et al. reported living-cell only bioinks. However, their supporting medium could not provide long-term support for 3D printed structures.[16] Instead of single cell-based bioprinting, there is a platform that permits skewering pre-cultured and formed multicellular aggregates on an array of needles to assemble structures of interest.[17] Cell strands, which are acquired by pre-culture and assembly of cells in a hollow fiber mold, have also been used as bioink for scaffold-free 3D bioprinting.[18] For these examples, the resolutions of the systems are limited by the original size and shape of the bioink cellular assemblies, preparing the bioinks demands additional time and expense, and neither permits printing of individual cells. Moreover, complicated instrumental setups required, such as vacuum syringe assisted skewering, may limit widespread implementation due to associated costs and necessary expertise.

Here, we present newly generated tissues from directly assembled stem cells, which have been 3D bioprinted into a photo-curable liquid-like supporting medium comprised of solid hydrogel microparticles (microgels) (Fig. S1 in ESI†). The supporting bath consists of biodegradable and photocrosslinkable alginate microgels, which are prepared by ionic crosslinking of dual-crosslinkable, oxidized and methacrylated alginate (OMA)[19], and is expected to applicable to general 3D bioprinting systems. The microgel supporting medium sustains the high-resolution printing of human bone marrow-derived mesenchymal stem cells (hMSCs) by exhibiting similar properties to Bingham plastic fluids.[20] While the microgel supporting medium allows the printing needle move freely via its shear-thinning properties, the microgels work as supporting materials for printed constructs through self-healing properties.[21] After directly 3D bioprinting of hMSCs into the microgel supporting medium, photocrosslinking of the microgels can provide mechanical stability for hMSC constructs for long-term culture. Dissociation of the photocrosslinked microgel supporting medium by gentle agitation may facilitate acquisition of matured 3D tissue constructs. Collectively, our objectives were (i) to assess the effect of the size of dual-crosslinkable OMA microgels in the supporting bath on printing resolution, (ii) to evaluate the capacity of the OMA supporting bath to maintain the viability individual printed cells and the structure of resulting self-assembly printed constructs, and (iii) to investigate function of the obtained 3D scaffold-free cellular constructs.

Results

3D bioprinting of living hMSCs without a biomaterial in the bioink

Living hMSCs can be printed as a bioink by themselves without a carrier macromer solution into a photo-curable, self-healing and shear-thinning alginate microgel supporting medium, which is formed with calcium-crosslinked OMA microgels (Fig. 1). Alginate microgel supporting medium is fluidized under low shear stress, permitting easy insertion and rapid motion of needles deep within the bulk. After removing shear stress caused by needle movement and ejection of printing material, the locally fluidized alginate microgel bath rapidly “self-heals” and forms a stable medium that firmly holds the printed hMSCs in 3D place (Fig. 1a). The low yield stress of the alginate microgel medium in its solid state and its rapid self-healing behavior allows the unrestricted deposition, placement and structuring of

cells deep within the alginate microgel supporting medium that maintains the printed structure with fidelity (Fig. 1b and Movie S1 and S2; The movies play at 4× speed.). To explore the versatility and stability of 3D printing into the alginate microgel supporting medium, a variety of complicated 3D structures were printed using only individual cells as a bioink. A letter (C), an ear, letters comprising an acronym (CWRU) and a femur were successfully created with high resolution (Fig. 1c–f). To demonstrate that this platform is amenable to 3D printing any cell type, human adipose-derived stem cells were printing in the form of a hand and a letter (C) and human dermal fibroblasts were printed into letters comprising the acronym “UIC” in the alginate microgel supporting medium (Fig. S2).

Properties of the alginate microgel supporting medium

To identify favorable properties of alginate microgels for use as supporting medium for 3D cell printing, several rheological measurements were performed on supporting medium made up of two different sizes of alginate microgels (Fig. 2 and Fig. S3 in ESI†). To verify the solid-like properties of alginate microgel supporting medium, a frequency sweep at low strain amplitude (1%) was conducted, measuring the elastic and viscous shear moduli and viscosity. The data show both sizes (7.0 ± 2.8 and 409.5 ± 193.7μm, Fig. S1 in ESI†) of alginate microgels behave like solid materials at low shear strain due to the steric stabilization of highly packed microgels (Fig. 2a and Fig. S3a in ESI†)[22], but they exhibit shear-thinning properties with decreased viscosity as shear rate increases (Fig. 2b and Fig S2b). To further identify the shear-thinning and shear yielding properties of the alginate microgel supporting medium in response to shear strain, the shear moduli with a strain sweep at a constant frequency (1Hz) was measured. Both sizes of OMA microgels exhibited shear-thinning (Fig. 2c and Fig. S3c in ESI†) and shear-yielding (Fig. 2d and Fig. S3d in ESI†) properties following increased shear strain application. Although both sizes of microgels exhibited a crossover at similar strain amplitude, the modulus at the crossover point (G’ = G”) of the smaller OMA microgels was much lower than that of the larger OMA microgels (Fig. 2d and Fig. S3d in ESI†). To characterize the self-healing or recovery behavior of the alginate microgel medium, dynamic strain tests were performed with alternate low (1%) and high (100%) strains. A rapid recovery of the storage modulus (Fig. 2e and Fig. S3e in ESI†) and viscosity (Fig. 2f and Fig. S3f) within seconds to the initial properties was repeatedly achieved over several cycles for both sizes of alginate microgels, indicating that the alginate microgel supporting medium can rapidly change from the solid to the fluid state via application of shear strain. Printing materials into viscoelastic supporting materials often results in crevasses created by the movement of the shaft of the dispensing needle and requires a third material that fills in crevasses.[23] However, 3D structures of hMSCs can be written into alginate microgel supporting medium without creating crevasses due to the self-healing properties of the alginate microgel supporting medium (Movie S3). To evaluate the capacity of the OMA microgels to provide long-term support for 3D printed constructs, frequency (at 1 % strain) and strain (at 1Hz) sweep tests were conducted after photocrosslinking of the smaller sized OMA microgel-based supporting medium under low-level UV light. Frequency (Fig. 2g) and strain (Fig. 2h) sweeps exhibited significantly higher G’ than G”, indicating that photocrosslinked OMA microgel supporting medium is mechanically stable without shear yielding. The stability of photocrosslinked OMA microgel supporting medium was also confirmed by a wash out test (Fig. S4 in ESI†). While the

photocrosslinked OMA microgel supporting medium remained stable on the Petri dish, uncrosslinked OMA microgel supporting medium could be easily removed by washing with water. The photocrosslinked OMA microgel supporting medium degraded over time and their degradation rate was controllable by changing the extent of alginate oxidation (Fig. S5).

Characterization of 3D printed cell-only filaments

Next, it was important to determine the minimum printed structure feature size achievable using this strategy. Lines or "filaments" of cells were printed into supporting medium with both sizes of alginate microgels to compare resulting resolutions. Regardless of the microgel size, hMSCs in filaments exhibited high cell viability as visualized by live/dead assay, demonstrating no adverse effects of the bioprinting process and UV irradiation for curing the microgel supporting medium on cell survival (Fig. 3a–c and e–f). The smaller alginate microgel supporting medium (Fig. 3d) exhibited higher resolution with narrow filament diameter distribution compared to the larger alginate microgel supporting medium (Fig. 3h), while the mean diameters of both hMSC filaments were similar (395.1 ± 64.6 and 419.8 ± 187.5 μm for filaments printed in small and larger microgel supporting medium, respectively). Since medium pores result from the space between the microgels, larger microgels make larger medium pores and vice versa. Due to the larger pores, many hMSCs printed into the larger alginate microgel supporting medium dispersed into the medium from the filaments, while hMSC filaments printed into the smaller alginate microgel supporting medium show a limited dispersion of cells. Therefore, 3D printed hMSC constructs in the smaller alginate microgel supporting medium (Fig. 3i and j) exhibit higher resolution than those in the larger alginate microgel supporting medium (Fig. 3k and l). These results indicate that the supporting medium comprised of smaller alginate microgels, which has lower stiffness, yield strength and viscosity, is more favorable for printing hMSCs with high resolution. Importantly, when cells were printed into the smaller alginate microgel supporting medium with smaller-gauge needles (25 and 27 G), significantly higher resolution of hMSC filaments ($p<0.05$, one-way ANOVA with Tukey's multiple comparison test using GraphPad Prism) was achieved (Fig. 3m–r) compared to that with the larger-gauge needle (Fig. 3a–c).

3D printing of complex structures and formation of engineered tissues

Long-term cell culture is essential to ensure tissue formation through maintenance cell-cell interactions, self-assembly into cellular condensations, and differentiation of the stem cells down desired lineages for engineering specific tissue types.[24] Critical to achieving this for a cell-only bioink is the capacity to provide the mechanical stability with the supporting medium during the culture period. Since the alginate microgels possess photo-reactive methacrylate groups (11 % actual methacrylation degree), the medium can be further photocrosslinked to form a more stable supporting structure that retains its shape for extended culture. After photocrosslinking, the alginate microgel supporting medium exhibited robust mechanical stability without shear yielding (Fig. 2h), maintained initial 3D printed structures (Fig. 1c–f) and enabled long-term culture of 3D printed constructs for formation of functional tissue by differentiation of 3D bioprinted hMSCs. After 4 weeks of osteogenic or chondrogenic differentiation, formed tissue constructs were easily harvested

from the alginate microgel supporting medium by applying shear force using a pipette. 3D printed hMSCs were assembled into precise multicellular structures with high cell viability (Fig. S6) following the architecture defined by computer-aided design (CAD) files (Fig. 4a and d), and bone- (Fig. 4b–c) or cartilage- (Fig. 4e–f and Fig. S7 in ESI†) like tissues were obtained in the photocrosslinked alginate microgel supporting medium. It was also possible to 3D print hMSC aggregates that fused and formed a cartilage-like tissue (Fig. S8). Differentiation down the osteogenic and chondrogenic lineages and resultant formation of bone and cartilage tissue were confirmed via Alizarin red (red) and Toluidine blue O (purple) staining, respectively; red and purple colors were intensively observed throughout the constructs (Fig. 4c and f) and sectioned samples (Fig. 4g and h). Lacunae structures were also observed in sectioned slides of chondrogenically differentiated constructs (Fig. 4h), indicating maturation of cartilage tissues.[25] Successful tissue formation by the 3D printed hMSCs were further confirmed by quantification of osteogenic (i.e., alkaline phosphatase (ALP) activity and calcium deposition) and chondrogenic (i.e., glycosaminoglycan (GAG) production) markers (Fig. S9 in ESI†). Collectively, the microgel supporting medium allows not only high-resolution printing of cell-only bioink, but also provides printed construct mechanical stability after additional photocrosslinking, which permits culture of the constructs with stable structural maintenance and long-term differentiation in differentiation medium.

Conclusions

To our knowledge, this is the first report of bioprinting strategy allowing the creation and maintenance of functional 3D engineered tissue structures using an individual cell-only bioink. Since the platform is applicable to universal 3D printers, it doesn't demand experts in either software or hardware fields[20]. Using a printing set-up costing <$1K, rapid construct formation on the centimeter scale was achieved in a few minutes, and even faster and more complex tissue printing with higher resolution may be accomplished with higher quality printers. As the microgel size decreased, it was possible to build tissue constructs with sophisticated structures due to the medium shear-thinning properties upon needle motion, self-healing properties in absence of external strain, and limited diffusion of the printed cells into its pores.[21] In addition, high viability of the printed cells was realized even after additional photocrosslinking of the microgels for long-term structural support. Unlike previous 3D bioprinting techniques which depend on external solid materials for structural maintenance or additional process for prefabrication of cell aggregates[17], the photocrosslinked OMA microgel supporting medium played a structural support role for the printed cell constructs, allowing media provision and long-term culture. Precise maintenance of the structure, mirroring the original CAD file design, was also achieved even after maturation of the tissue which possibly caused deformation, shrinking and/or thickening of the printed constructs due to cell proliferation, differentiation and ECM production.[26] Since the OMA microparticles can be removed by simple agitation or spontaneous degradation from the constructs, the cultured constructs can be easily harvested from the alginate microgel supporting medium without damage. This universally applicable 3D printing platform makes it possible to print isolated cells without a biomaterial carrier in the bioink, and will contribute to regenerative medicine by permitting generation of biomimetic cellular

condensation-based engineered tissues with defined geometries comprised of multiple cell types with controlled spatial placement.

Supplementary Material

Refer to Web version on PubMed Central for supplementary material.

Acknowledgement

The authors thank Dr. Kent J. Leach at the University of California, Davis, for providing the PDMS microwell molds and Julia Samorezov at Case Western Reserve University for providing the hASCs. The authors gratefully acknowledge funding from the National Institutes of Health's National Institute of Arthritis and Musculoskeletal and Skin Diseases under award numbers R01AR063194 and R01AR066193 and National Institute of Biomedical Imaging and Bioengineering under award number R01EB023907. The contents of this publication are solely the responsibility of the authors and do not necessarily represent the official views of the National Institutes of Health.

References

1. Mao AS, Mooney DJ, Proceedings of the National Academy of Sciences of the United States of America, 2015, 112, 14452–14459. [PubMed: 26598661]
2. Norotte C, Marga FS, Niklason LE, Forgacs G, Biomaterials, 2009, 30, 5910–5917. [PubMed: 19664819]
3. Ovsianikov A, Khademhosseini A, Mironov V, Trends in biotechnology, 2018, 36, 348–357. [PubMed: 29475621]
4. Dikina AD, Alt DS, Herberg S, McMillan A, Strobel HA, Zheng Z, Cao M, Lai BP, Jeon O, Petsinger VI, Cotton CU, Rolle MW, Alsberg E, Advanced science, 2018, 5, 1700402. [PubMed: 29876200]
5. Li PY, Shi Q, Wang HP, Tu XL, Sun T, Liu XM, Huang Q, Fukuda T, 2015 Ieee International Conference on Robotics and Biomimetics (Robio), 2015, 1967–1972.
6. Souza GR, Molina JR, Raphael RM, Ozawa MG, Stark DJ, Levin CS, Bronk LF, Ananta JS, Mandelin J, Georgescu MM, Bankson JA, Gelovani JG, Killian TC, Arap W, Pasqualini R, Nature nanotechnology, 2010, 5, 291–296.
7. Mandrycky C, Wang Z, Kim K, Kim DH, Biotechnology advances, 2016, 34, 422–434. [PubMed: 26724184]
8. Song KH, Highley CB, Rouff A, Burdick JA, Adv Funct Mater, 2018, 28, 1801331.
9. Lee H, Rodeo SA, Fortier LA, Lu CY, Erisken C, Mao JJ, Sci Transl Med, 2014, 6, 1–11.
10. Gregor A, Filova E, Novak M, Kronek J, Chlup H, Buzgo M, Blahnova V, Lukasova V, Bartos M, Necas A, Hosek J, Journal of biological engineering, 2017, 11, 31. [PubMed: 29046717]
11. Guo T, Holzberg TR, Lim CG, Gao F, Gargava A, Trachtenberg JE, Mikos AG, Fisher JP, Biofabrication, 2017, 9, 024101. [PubMed: 28244880]
12. Cui H, Nowicki M, Fisher JP, Zhang LG, Advanced healthcare materials, 2017, 6, 1601118.
13. Radhakrishnan J, Subramanian A, Krishnan UM, Sethuraman S, Biomacromolecules, 2017, 18, 1–26. [PubMed: 27966916]
14. Hinton TJ, Jallerat Q, Palchesko RN, Park JH, Grodzicki MS, Shue HJ, Ramadan MH, Hudson AR, Feinberg AW, Sci Adv, 2015, 1, e1500758. [PubMed: 26601312]
15. Highley CB, Rodell CB, Burdick JA, Adv Mater, 2015, 27, 5075–5079. [PubMed: 26177925]
16. Bhattacharjee T, Gil CJ, Marshall SL, Uruena JM, O'Bryan CS, Carstens M, Keselowsky B, Palmer GD, Ghivizzani S, Gibbs CP, Sawyer WG, Angelini TE, Acs Biomater Sci Eng, 2016, 2, 1787–1795.
17. Ong CS, Fukunishi T, Zhang H, Huang CY, Nashed A, Blazeski A, DiSilvestre D, Vricella L, Conte J, Tung L, Tomaselli GF, Hibino N, Scientific reports, 2017, 7, 4566. [PubMed: 28676704]
18. Yu Y, Moncal KK, Li JQ, Peng WJ, Rivero I, Martin JA, Ozbolat IT, Scientific reports, 2016, 6, 28714. [PubMed: 27346373]

19. Jeon O, Alt DS, Ahmed SM, Alsberg E, Biomaterials, 2012, 33, 3503–3514. [PubMed: 22336294]
20. Hinton TJ, Hudson A, Pusch K, Lee A, Feinberg AW, Acs Biomater Sci Eng, 2016, 2, 1781–1786. [PubMed: 27747289]
21. O'Bryan CS, Bhattacharjee T, Hart S, Kabb CP, Schulze KD, Chilakala I, Sumerlin BS, Sawyer WG, Angelini TE, Sci Adv, 2017, 3, e1602800 [PubMed: 28508071]
22. Berli CLA, Quemada D, Langmuir, 2000, 16, 7968–7974.
23. Wu W, DeConinck A, Lewis JA, Adv Mater, 2011, 23, 178–183.
24. Guilak F, Cohen DM, Estes BT, Gimble JM, Liedtke W, Chen CS, Cell Stem Cell, 2009, 5, 17–26. [PubMed: 19570510]
25. Dikina AD, Almeida HV, Cao M, Kelly DJ, Alsberg E, Acs Biomater Sci Eng, 2017, 3, 1426–1436.
26. Visscher DO, Bos EJ, Peeters M, Kuzmin NV, Groot ML, Helder MN, van Zuijlen PP, Tissue engineering. Part C, Methods, 2016, 22, 573–584. [PubMed: 27089896]

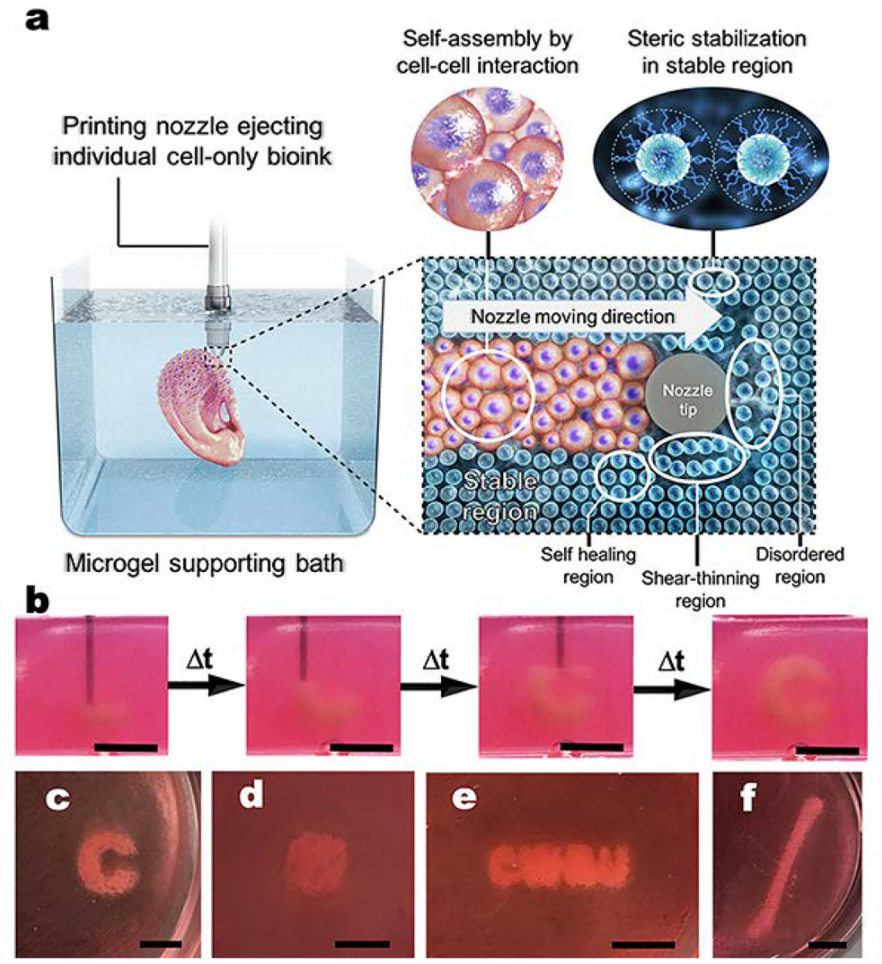

Fig. 1. Shear-thinning and self-healing alginate microgel supporting medium for 3D bioprinting of living individual stem cells.

(a) A schematic of 3D printing of cells within the alginate microgel supporting medium. OMA microgels in the supporting medium fluidize via their shear-thinning properties when stress is applied by motion of the printing needle and cell-only bioink (shear-thinning region) and rapidly fill in after the needle passes by self-healing properties (self-healing region) without creating crevasses. Microgel supporting medium without shear stress presents solid-like properties, which provide mechanical stability for the printed cell construct (stable region). **(b)** Captured images at different times during bioprinting of the letter “C” using living stem cell-only bioink into the alginate microgel supporting medium. As the printing progress, cells are arranged into the letter “C” shape in 3D without disturbing previously printed regions, which is achieved as a result of the shear-thinning and self-healing properties of the alginate microgel supporting medium. Images of the 3D bioprinted structures of **(c)** a letter “C”, **(d)** a cube, **(e)** letters comprising the acronym “CWRU”, and **(f)** a femur in alginate microgel supporting medium. Scale bars indicate 5 mm.

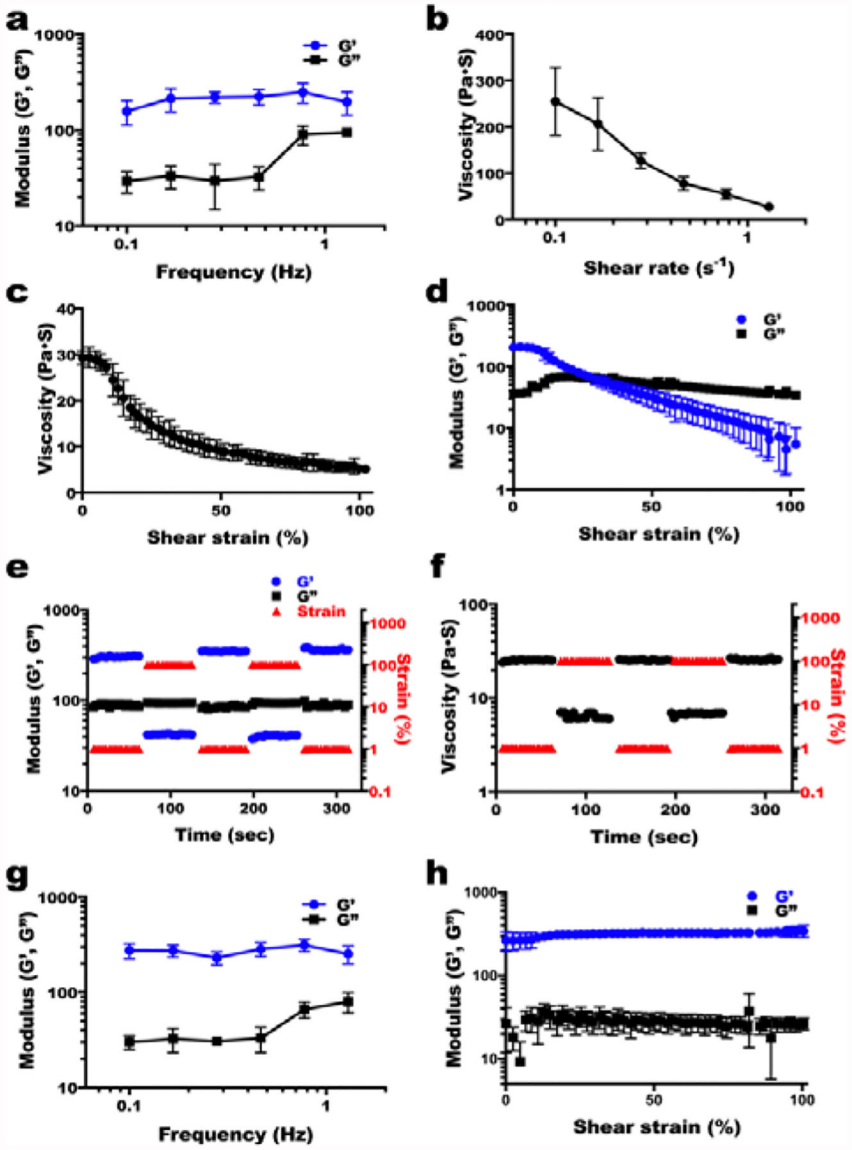

Fig. 2. Shear-thinning and self-healing properties of the alginate microgel supporting medium.

(a) Storage (G') and loss (G") moduli of alginate microgel supporting medium (mean microgel diameter = 7.0 ± 2.8 μm) as a function of frequency. G' is larger than G" over the measured frequency range and both moduli exhibit frequency independence. Viscosity measurements of alginate microgel supporting medium as a function of **(b)** shear rate and **(c)** shear strain demonstrate its shear-thinning behavior. **(d)** G' and G" of the alginate microgel supporting medium as a function of shear strain exhibit its shear-yielding behavior and gel-to-sol transition at higher shear strain. **(e)** Shear moduli and **(f)** viscosity changes in dynamic strain tests of the alginate microgel supporting medium with alternating low (1%) and high (100%) strains at 1 Hz demonstrate its rapid recovery of strength and viscosity within seconds, which indicates "self-healing" or thixotropic properties. **(g)** Frequency sweep (at 1 % strain) and **(h)** strain sweep (at 1 Hz) tests of the alginate microgel supporting medium after photocrosslinking under low-level UV light. G' is larger than G" over the measured

frequency and strain ranges and both moduli exhibit frequency and strain independence, indicating that the photocrosslinked alginate microgel supporting medium is mechanically stable.

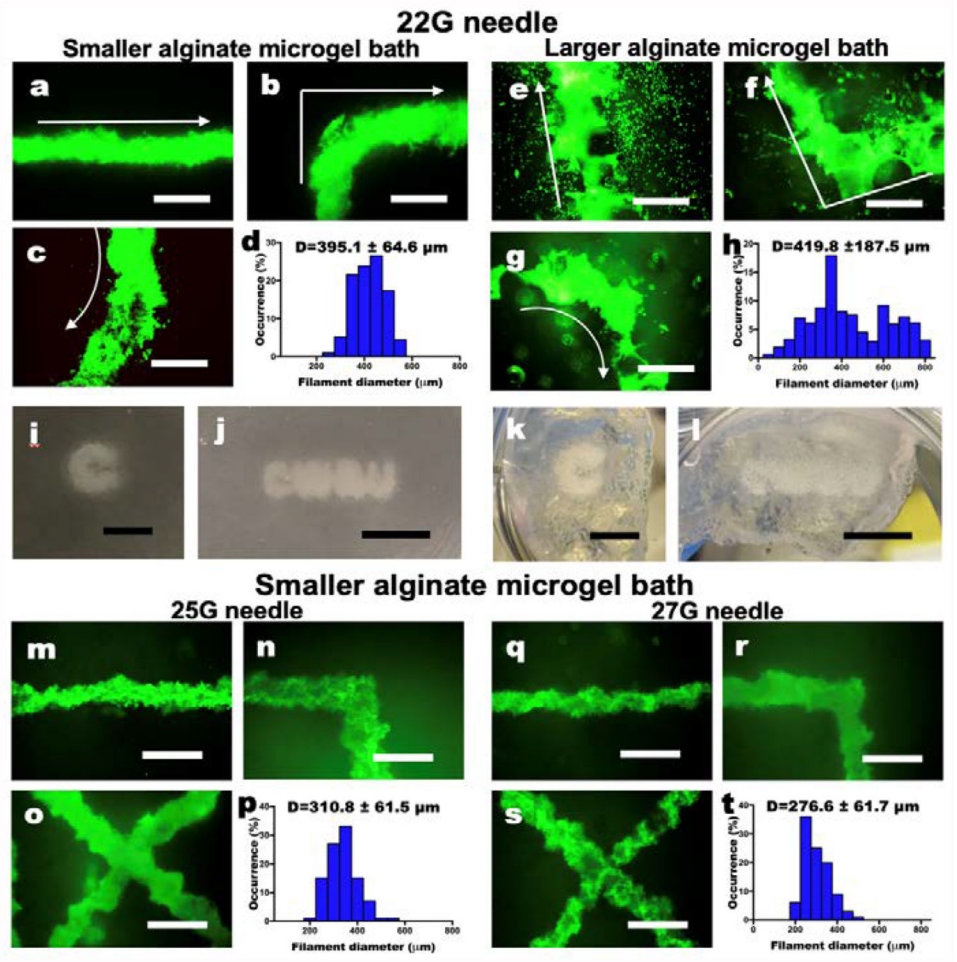

Fig. 3. Characterization of living cell-only bioink.

(a-c) Live/Dead staining of 3D hMSC filaments bioprinted in a straight line, a corner and a curve with a **22 G** needle and **(d)** their diameter distribution in **the smaller alginate microgel supporting medium**. **(e-g)** Live/Dead staining of 3D hMSC filaments bioprinted in various configurations with a **22 G** needle and **(h)** their diameter distribution in **the larger alginate microgel supporting medium**. Arrows indicate the direction of movement of the printing nozzle. Scale bars indicate 600 μm. The Live/Dead images demonstrate high cell viability. Smaller alginate microgels lead to higher resolution printing by limiting diffusion of cells into the pores of the microgel bath. Thickness of the cell filaments also are more narrowly distributed in smaller microgel medium. Images of letters ‘C’ and “CWRU” in **(i and j)** the smaller and (**k and l)** larger alginate microgel supporting medium after photocrosslinking. Scale bars indicate 5 mm. **(m-o)** Live/Dead staining of 3D hMSC filaments bioprinted in various configurations with a **25 G** needle and **(p)** their diameter distribution in **the smaller alginate microgel supporting medium**. **(q-s)** Live/Dead staining of 3D hMSC filaments bioprinted in various configurations with a **27 G** needle and **(h)** their diameter distribution in **the smaller alginate microgel supporting medium**. Scale bars indicate 600 μm. Smaller diameter needles lead to higher resolution printing of the cell filaments, which also are more narrowly distributed. Scale bars indicate 600 μm.

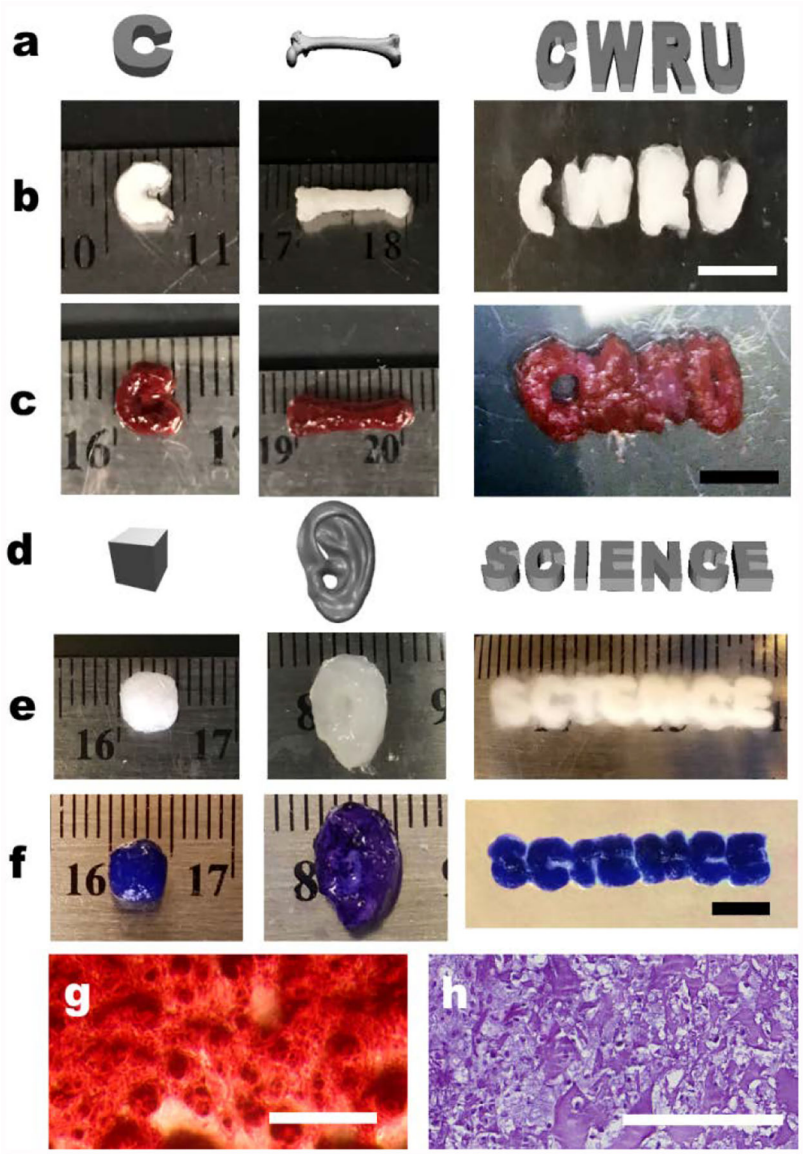

Fig. 4. Differentiation of 3D bioprinted hMSC constructs.

(a) Digital images and photographs of osteogenically differentiated 3D printed individual hMSC-only bioink construct morphology **(b)** before and **(c)** after Alizarin red S staining. Scale bars indicate 5 mm. **(d)** Digital images and photographs of chondrogenically differentiated 3D printed hMSC construct morphology **e)** before and **(f)** after Toluidine blue O staining. The constructs presented well-preserved structures after long-term 4- week culture without evidence of construct deformation due to cellular contraction or proliferation, and generation of specific tissue types (i.e., bone and cartilage) with desired geometries. Scale bar indicates 5 mm. Photomicrographs of **(g)** Alizarin Red S and **(h)** Toluidine Blue O stained construct sections. The images demonstrate hMSC differentiation and deposition of lineage specific ECM in the cell-only bioink printed constructs. Scale bars indicate 200 μm.